

## ORIGINAL ARTICLE

# A robust nitrifying community in a bioreactor at 50 °C opens up the path for thermophilic nitrogen removal

Emilie NP Courtens<sup>1</sup>, Eva Spieck<sup>2</sup>, Ramiro Vilchez-Vargas<sup>1</sup>, Samuel Bodé<sup>3</sup>, Pascal Boeckx<sup>3</sup>, Stefan Schouten<sup>4</sup>, Ruy Jauregui<sup>5</sup>, Dietmar H Pieper<sup>5</sup>, Siegfried E Vlaeminck<sup>1,6,7</sup> and Nico Boon<sup>1,7</sup>

<sup>1</sup>Laboratory of Microbial Ecology and Technology (LabMET), Ghent University, Gent, Belgium; <sup>2</sup>Biocenter Klein Flottbek and Department of Microbiology and Biotechnology, University of Hamburg, Hamburg, Germany; <sup>3</sup>Isotope Bioscience Laboratory, Ghent University, Gent, Belgium; <sup>4</sup>Royal Netherlands Institute for Sea Research (NIOZ), Texel, The Netherlands; <sup>5</sup>Microbial Interactions and Processes Research Group, Helmholtz Centre for Infection Research, Braunschweig, Germany and <sup>6</sup>Research Group of Sustainable Energy, Air and Water Technology, University of Antwerp, Antwerpen, Belgium

**The increasing production of nitrogen-containing fertilizers is crucial to meet the global food demand, yet high losses of reactive nitrogen associated with the food production/consumption chain progressively deteriorate the natural environment. Currently, mesophilic nitrogen-removing microbes eliminate nitrogen from wastewaters. Although thermophilic nitrifiers have been separately enriched from natural environments, no bioreactors are described that couple these processes for the treatment of nitrogen in hot wastewaters. Samples from composting facilities were used as inoculum for the batch-wise enrichment of thermophilic nitrifiers (350 days). Subsequently, the enrichments were transferred to a bioreactor to obtain a stable, high-rate nitrifying process (560 days). The community contained up to 17% ammonia-oxidizing archaea (AOAs) closely related to ‘*Candidatus Nitrososphaera gargensis*’, and 25% nitrite-oxidizing bacteria (NOBs) related to *Nitrospira calida*. Incorporation of <sup>13</sup>C-derived bicarbonate into the respective characteristic membrane lipids during nitrification supported their activity as autotrophs. Specific activities up to 198 ± 10 and 894 ± 81 mg N g<sup>-1</sup> VSS per day for AOAs and NOBs were measured, where NOBs were 33% more sensitive to free ammonia. The NOBs were extremely sensitive to free nitrous acid, whereas the AOAs could only be inhibited by high nitrite concentrations, independent of the free nitrous acid concentration. The observed difference in product/substrate inhibition could facilitate the development of NOB inhibition strategies to achieve more cost-effective processes such as deammonification. This study describes the enrichment of autotrophic thermophilic nitrifiers from a nutrient-rich environment and the successful operation of a thermophilic nitrifying bioreactor for the first time, facilitating opportunities for thermophilic nitrogen removal biotechnology.**

*The ISME Journal* (2016) 10, 2293–2303; doi:10.1038/ismej.2016.8; published online 19 February 2016

## Introduction

The increased combustion of fossil fuels and extensive production of nitrogen-containing fertilizers and industrial products lead to accumulation of reactive nitrogen in many natural ecosystems, causing a worldwide environmental problem (Galloway *et al.*, 2014). As with biodiversity loss and climate change, the aforementioned anthropogenic distortion of the nitrogen cycle has by far exceeded the safety

boundaries of our planet (Steffen *et al.*, 2015). Nitrification, the two-step microbe-mediated aerobic oxidation of ammonia to nitrate, plays a key role in the transformation of reactive nitrogen necessary to restore the imbalanced nitrogen cycle. Ammonia-oxidizing bacteria (AOBs) and archaea (AOAs) catalyze the first step, that is, the oxidation of ammonia (NH<sub>3</sub>) to nitrite (NO<sub>2</sub><sup>-</sup>), whereas the successive oxidation to nitrate (NO<sub>3</sub><sup>-</sup>) is carried out by nitrite-oxidizing bacteria (NOBs).

Most AOBs grow optimally at temperatures between 25 °C and 30 °C (Ward *et al.*, 2011), with a maximum reported growing temperature of 55 °C (Lebedeva *et al.*, 2005). The recent discovery of ‘*Candidatus Nitrosocaldus yellowstonii*’, an archaeon that grows up to 74 °C, however broadened the phylogenetic spectrum of ammonia oxidizers active at high temperatures (de la Torre *et al.*, 2008).

Correspondence: N Boon, Laboratory of Microbial Ecology and Technology (LabMET), Ghent University, Coupure Links 653, Gent 9000, Belgium.

E-mail: Nico.Boon@UGent.be

<sup>7</sup>These authors contributed equally and are both senior authors for this work.

Received 9 April 2015; revised 3 January 2016; accepted 4 January 2016; published online 19 February 2016

Two other moderately thermophilic (46 °C) AOA ‘*Candidatus Nitrososphaera gargensis*’ (Hatzenpichler *et al.*, 2008) and ‘*Candidatus Nitrosotenuis uzonensis*’ (Lebedeva *et al.*, 2013) have been enriched from Russian hot springs. Thermophilic ammonia oxidation is fueling hydrothermal and geothermal life. Many archaeal ammonia monooxygenase subunit A (*amoA*) genes have been detected in high-temperature habitats such as deep-sea hydrothermal vents (Wang *et al.*, 2009; Baker *et al.*, 2012), subsurface thermal springs (Spear *et al.*, 2007; Weidler *et al.*, 2008) and terrestrial hot springs (Reigstad *et al.*, 2008; Dodsworth *et al.*, 2011). In addition to these oligotrophic ecosystems, the *amoA* gene was also found in nutrient-rich high-temperature engineered environments such as petroleum reservoirs (Li *et al.*, 2011) and composting facilities (Zeng *et al.*, 2011). Although many archaeal *amoA* genes were detected in thermophilic environments, only three enrichments have been described so far (‘*Candidatus Nitrosocaldus. yellowstonii*’, ‘*Candidatus Nitrososphaera gargensis*’ and ‘*Candidatus Nitrosotenuis uzonensis*’).

Regarding thermophilic nitrite oxidation, it appears that *Nitrospira* spp. are the dominant  $\text{NO}_2^-$  oxidizers up to 60 °C. *Nitrospira calida* was isolated from a microbial mat of a terrestrial geothermal spring and maximally oxidizes  $\text{NO}_2^-$  at 46–52 °C (Lebedeva *et al.*, 2011). Thus far, other detected/enriched NOBs from geothermal springs are all closely related with *N. calida* (Marks *et al.*, 2012; Edwards *et al.*, 2013).

Thermophilic microorganisms played a crucial role during the evolution of life on our planet (Nisbet and Sleep, 2001). Despite the partnership between AOA and *Nitrospira* spp. that potentially pioneered in ancestral nitrification (Vlaeminck *et al.*, 2011), until now, thermophilic nitrifiers were always separately enriched/studied in batch cultures. Coupled ammonia and nitrite oxidation under thermophilic conditions has not yet been described, neither in long-term batch flask enrichments nor in bioreactors. Except for the recently described *Nitrolancea hollandica* (Sorokin *et al.*, 2014), all reported substrate/product inhibitions levels for the described thermophilic nitrogen-converting organisms are relatively low (Hatzenpichler *et al.*, 2008; Lebedeva *et al.*, 2011), making them rather unsuitable for robust biotechnological applications. Lopez-Vazquez *et al.* (2014) recently reported nitrifying activity up to 50 °C in mesophilic sludge from an industrial wastewater treatment plant after temperature shocking of mesophilic biomass (34 °C) in short-term batch activity assays. However, the observations by Courtens *et al.* (2014a) pointed out that prolonged exposure (48 h) of mesophilic biomass to a temperature shock can lead to a complete loss of nitrifying activity. To our knowledge, there is no description of nitrification at 50 °C or above for an extended period of time. Long-term thermophilic aerobic bioreactor studies focused mainly on the oxidation of organic

compounds. The major nitrogen removal mechanisms in those systems were assumed to be ammonia volatilization ( $65 \pm 14\%$ ) and nitrogen assimilation into biomass ( $14 \pm 4$ ) (Yi *et al.*, 2003; Kurian *et al.*, 2005; Abeynayaka and Visvanathan, 2011a, b). As neither nitrite nor nitrate was ever measured in these bioreactors at 45–60 °C, there is no evidence that nitrification took place in these thermophilic systems. Until now, only a few bioreactor studies focused on the long-term establishment of coupled thermophilic ammonia and nitrite oxidation, yet reaching no more than 42 °C (Shore *et al.*, 2012; Courtens *et al.*, 2014a).

This study describes the enrichment of autotrophic thermophilic nitrifiers from compost and the successful operation of a thermophilic nitrifying bioreactor with high biotechnological potential. We demonstrate that autotrophic AOA and NOBs serve as key players in the microbial community of the thermophilic nitrifying bioreactor. We also provide a phylogenetic, physiological and morphological characterization of this unique nitrifying consortium.

## Materials and methods

### *Inoculum and batch enrichments*

Different aerobic compost facilities were sampled during the thermophilic stage (50–70 °C): digested organic waste (a), green waste (b), cow manure (c) and a mix of rabbit manure/green waste (d). A ‘compost extract’ was prepared by shaking 20 g of compost in 200 ml water with glass beads (12 h). The extract was used as inoculum (25 vol%) for enrichment incubations (50 °C) in a buffered medium (pH 7) with final concentrations of 0.929 g  $\text{KH}_2\text{PO}_4 \text{ l}^{-1}$ , 1.622 g  $\text{K}_2\text{HPO}_4 \text{ l}^{-1}$  and 0.5 g  $\text{NaHCO}_3 \text{ l}^{-1}$  with  $(\text{NH}_4)_2\text{SO}_4$  or  $\text{NaNO}_2$  as the only substrate (20 mg  $\text{N l}^{-1}$ ). All incubations were provided with two different packing materials, K1 carriers (Anox-Kaldnes (Veolia), Saint-Maurice, France) and polyurethane foam (Shenzhen Lianda, Guangdong, China), to allow for both floccular and biofilm growth.

### *Reactor set-up and operation*

The compost enrichments showing both  $\text{NH}_3$  and  $\text{NO}_2^-$  oxidation (b, d) were transferred to a bioreactor. The reactor vessel (2 l, diameter 12 cm) was jacketed, allowing temperature control at 50 °C with a circulating thermostatic water bath. The reactor was operated in a sequencing batch feeding/withdrawal mode. The 3 h cycle consisted of a 150-min aerobic reaction period, a 10-min feeding period at the beginning of the cycle, a 15-min settling period, a 5-min decanting period and a 10-min idle period. The bioreactor was fed with a synthetic medium consisting of  $(\text{NH}_4)_2\text{SO}_4$  (10–140 mg  $\text{N l}^{-1}$ ),  $\text{NaNO}_2$  (0–50 mg  $\text{N l}^{-1}$ ), 9 g  $\text{NaHCO}_3 \text{ g}^{-1} \text{N}$ ,  $\text{KH}_2\text{PO}_4$  (10 mg  $\text{P l}^{-1}$ ),  $\text{NaCl}$  (1.2 g  $\text{l}^{-1}$ ) and 0.1 ml  $\text{l}^{-1}$  trace

element solution (Kuai and Verstraete, 1998) dissolved in tap water. A flow rate of  $3.4 \pm 0.2 \text{ l d}^{-1}$  resulted in a hydraulic retention time of  $14 \pm 0.7 \text{ h}$ . Any transient  $\text{NH}_4^+/\text{NO}_2^-$  build-up was immediately corrected by adjusting the nitrogen loading, preventing accumulation of free ammonia (FA) or free nitrous acid (FNA). The reactor pH was controlled between pH 6.8 and 7.2 by a dosage of 0.1 M NaOH/HCl. The dissolved oxygen was controlled at  $3.6 \pm 0.2 \text{ mg l}^{-1}$  with air pumps providing aeration through a diffuser stone at a superficial air flow rate of  $1.33 \text{ m}^3 \text{ m}^{-2} \text{ h}^{-1}$ .

#### Physiological characterization

Physiological characterization along with inhibition tests were performed in *ex situ* batch activity measurements in 96-well plates with a working volume of 250  $\mu\text{l}$ . Plates were incubated in a MB100-4A Thermoshaker (Hangzhou Allsheng Instruments, Hangzhou, China) at 50 °C and 600 r.p.m., containing a buffer solution with a final concentration of  $500 \text{ mg P l}^{-1}$  ( $\text{KH}_2\text{PO}_4/\text{K}_2\text{HPO}_4$ ),  $500 \text{ mg NaHCO}_3 \text{ l}^{-1}$ ,  $0.1 \text{ ml l}^{-1}$  trace element solution (Kuai and Verstraete 1998) and  $(\text{NH}_4)_2\text{SO}_4$  or  $\text{NaNO}_2$ .

Operational parameters in the batch tests varied according to the investigated parameter. The pH, temperature and substrate concentrations were measured in all tests. From these, FA/FNA concentrations were calculated based on their chemical equilibrium (Anthonisen *et al.*, 1976). The effects of the different parameters can only be separated from each other by a combination of different tests as presented in Supplementary Table S1 for ammonia oxidation. A similar strategy was applied for separation of nitrite and FNA effects on nitrite oxidation (Supplementary Table S2). All treatments were performed in sextuple, and liquid samples (2  $\mu\text{l}$ ) were taken over time for  $\text{NH}_4^+$  and  $\text{NO}_2^-$  analysis. Protein measurements enabled the calculation of specific rates that were converted to volatile suspended solids (VSS) based on the average protein content of the thermophilic sludge (32.7% protein per VSS).

#### High-throughput DNA sequencing, phylogenetic analysis and quantitative PCR

Biomass samples of the reactor were collected over time, and total DNA was extracted as described previously (Courtens *et al.*, 2014b). Prokaryotic biodiversity was analyzed using pair-end high-throughput sequencing (MiSeq Illumina platform, San Diego, CA, USA) of the regions V5–V6 of the 16S rRNA gene, using the primers 807F and 1050R as previously described (Bohorquez *et al.*, 2012). Libraries for barcoding sequencing were constructed as previously described (Camarinha-Silva *et al.*, 2014). The sequences were analyzed, obtaining 189 358 total reads of 240 nucleotides in length. After a quality filter, 153 611 total operational taxonomic units (OTUs) were obtained and clustered

into 155 unique taxa (Camarinha-Silva *et al.*, 2014). Forward and reverse reads were aligned manually, allowing zero mismatch (Supplementary Data Set S1). Each set of reads was normalized to the minimum sequencing depth, obtaining 18 191 OTUs per sample. The 163 unique taxa were taxonomically annotated manually (Supplementary Data Set S1). The vegan and phyloseq packages in the statistical software R (The R Foundation, Vienna, Austria) were used to plot the rarefaction curves and normalize to the minimum sequencing depth respectively. Phylogenetic analyses were performed with MEGA5 (Tamura *et al.*, 2011). The evolutionary history was inferred by using the maximum likelihood method based on the Jukes–Cantor model (Jukes and Cantor, 1969) and the percentage of trees in which the associated taxa clustered together is shown next to the branches. In total, 1000 bootstrap replications were performed to test for branch robustness. The heat map was generated using gplots and RColorBrewer packages. The SYBR Green assay (Power SyBr Green, Applied Biosystems, Carlsbad, CA, USA) was used to quantify the 16S rRNA of *Nitrospira* spp. (Dionisi *et al.*, 2002) and the functional archaeal *amoA* gene (Tournai *et al.*, 2008).

#### Electron microscopy

For electron microscopy, biofilm material from three different sampling points in the bioreactor was fixated and embedded in SPURR as described by Spieck and Lipski (2011). The ultrathin sections were observed using a transmission electron microscope (model JEM 100C or LEO-906E, Zeiss, Jena, Germany).

#### Stable isotope probing: membrane lipids

Reactor biomass was incubated (50 °C, 100 r.p.m.) in 120 ml gas-tight serum flasks containing 20 ml phosphate buffer (pH 7) with final concentrations of  $750 \text{ mg P l}^{-1}$  ( $\text{KH}_2\text{PO}_4/\text{K}_2\text{HPO}_4$ ),  $1 \text{ g NaH}^{13}\text{CO}_3 \text{ l}^{-1}$  and  $\text{NH}_4^+$  or  $\text{NO}_2^-$  as the sole nitrogen source. Liquid samples (2  $\mu\text{l}$ ) were taken over time for  $\text{NH}_4^+$  and  $\text{NO}_2^-$  analysis. The pH was adjusted through the addition of HCl or  $\text{NaH}^{13}\text{CO}_3$ . Biomass from three parallel incubations with  $\text{NH}_4^+$  (harvested at days 0, 49 and 85) served for alkyl iodides analysis, whereas biomass from five parallel incubations with  $\text{NO}_2^-$  (harvested at days 0, 3, 7, 14 and 21) served for phospholipid fatty acid analysis. The sampling points were determined based on the relative abundance of the AOAs/NOBs, the oxidation rates and the sensitivity of the respective biomarker analysis.

*Alkyl iodides analysis.* Biomass was subjected to acid hydrolysis by refluxing for 3 h with 5% HCl in MeOH. The resulting extract was separated using  $\text{Al}_2\text{O}_3$  chromatography. Hexane/dichloromethane (9:1) and dichloromethane/methanol (1:1) were used as eluents, yielding an apolar and polar fraction. An aliquot of the polar fraction was analyzed for

tetraether lipids using high-performance liquid chromatography/mass spectrometry (Schouten *et al.*, 2007). The remaining polar fractions were subjected to chemical treatment to release the biphytanyl chains from the tetraether lipids (Lengger *et al.*, 2014). The stable carbon isotopic composition of the released biphytanes was analyzed in replicate using an Agilent 6800 GC coupled to a Thermo Fisher Delta V isotope ratio monitoring mass spectrometer (Thermo Fisher Scientific, Waltham, MA, USA) (Lengger *et al.*, 2014).

**Phospholipid fatty acid analysis.** Extraction and derivatization of phospholipid fatty acids for compound-specific  $^{13}\text{C}$  analysis was adapted from Huygens *et al.* (2011). Identification of 11-methyl C16:0 was based on the retention time and comparison with published mass spectra (Lipski *et al.*, 2001) using the mass fragments  $m/z$  185 and  $m/z$  213 resulting from cleavage of the molecule at both sides of the methyl branch, as these are diagnostic fragments of 11-methyl-branched fatty acid methyl ester. Isotopic enrichment was assessed using the  $m/z$  74/(74+76) ratio of the methyl acetate ion fragment.

#### Chemical analyses

$\text{NH}_4^+$  (Nessler method) and VSS were measured according to standard methods.  $\text{NO}_2^-$  and  $\text{NO}_3^-$  were determined on a 930 Compact Ion Chromatograph (Metrohm, Herisau, Switzerland) equipped with a conductivity detector. Dissolved oxygen and pH levels were measured with an Oxymax COS22D probe (Endress Hauser, Reinach, Switzerland) and a Dulcotest pH-electrode PHEP 112 SE (Prominent, Heidelberg, Germany), respectively. In the batch activity tests,  $\text{NH}_4^+$  and  $\text{NO}_2^-$  concentrations were determined spectrophotometrically with the Berthelot and Montgomery reaction. Measurements were obtained using a Tecan infinite plate reader (Tecan, Männedorf, Switzerland), and biomass was quantified through protein concentrations. To determine the protein concentration, the method developed by Lowry was used with bovine serum albumin as the standard.

## Results

#### Thermophilic batch enrichments

Samples from four composting facilities served as inocula for the batch-wise enrichment of thermophilic (50 °C) nitrifying communities. The different origin of the organic fractions and different compost process parameters (temperature, pH) resulted in different nitrogen compound distributions in the four compost solutions. The mineralized nitrogen in the green waste (a) and rabbit manure/green waste mixture (b) constituted oxidized forms of nitrogen ( $\text{NO}_2^-/\text{NO}_3^-$ ), whereas  $\text{NH}_4^+$  was the only form of inorganic nitrogen in the digested organic waste (c)

and cow manure (d) (Supplementary Table S3). This distinction was reflected in the observed thermophilic nitrifying activity. First,  $\text{NH}_3$  and  $\text{NO}_2^-$  oxidation was observed after  $\sim 100$  days of incubation. Samples (a) and (b) showed both  $\text{NH}_4^+$  and  $\text{NO}_2^-$  oxidation, whereas samples (c) and (d) only showed  $\text{NO}_2^-$  oxidation. After 1 year of incubation and several re-inoculation steps into fresh medium, two highly active nitrite-oxidizing and two coupled ammonia- and nitrite-oxidizing enrichment communities were obtained (Supplementary Figure S1).

#### Bioreactor performance

The enrichments showing complete nitrification were pooled and served as inoculum for the bioreactor at 50 °C. Initial volumetric nitrification rates were low ( $4.7 \pm 2.6 \text{ mg N l}^{-1} \text{ d}^{-1}$ ). However, after 2 months of operation, a clear exponential increase in nitrifying activity was observed in the reactor reaching volumetric  $\text{NH}_3$  and  $\text{NO}_2^-$  oxidation rates of  $126 \pm 7$  and  $189 \pm 17 \text{ mg N l}^{-1} \text{ d}^{-1}$ , respectively (Figure 1). After this first stage, because of a technical failure, the community was challenged by a temperature drop to 30 °C and a subsequent shock at pH 11 (days 235–238), leading to an initial loss of ammonia oxidation activity. However, the reactor restabilized successfully, reaching nitrification rates higher than  $200 \text{ mg NH}_4^+ \text{ N l}^{-1} \text{ d}^{-1}$  (Figure 1). Practically all the removed  $\text{NH}_4^+ \text{ N}$  was recovered as  $\text{NO}_3^- \text{ N}$  ( $93 \pm 4\%$ ), confirming that nitrification was the main process involved. The biomass predominantly appeared as an orange to brownish biofilm on the packing material and wall of the reactor vessel.

#### Phylogeny and morphology

The thermophilic nitrifying microbial community was analyzed once in the first stage (day 150, data not shown) and once during the restabilization period of the reactor (days 245–387). Illumina sequencing identified one unique sequence (OTU7) of archaea closely related to the AOA 'Candidatus Nitrososphaera gargensis' Ga9.2 (99% similarity) (Figure 2), whereas no known AOB could be detected. For nitrite oxidation, several different sequences closely related to *Nitrospira* spp. were identified. OTU1, 99% similar to the *N. calida* Ns10 16S rRNA gene sequence (Figure 3), was the most abundant *Nitrospira* sequence in the *Nitrospira* community ( $98 \pm 2\%$ ) and the only *Nitrospira*-related OTU that strongly increased in abundance over time (Supplementary Figure S2). Both Illumina sequencing and quantitative PCR analyses showed a considerable increase in abundance of *Nitrospira*-related NOBs and archaeal ammonia oxidizers over 6 months of operation (Supplementary Figure S3). The higher relative abundance of NOB ( $\pm 25\%$  vs.  $\pm 10\%$ ) in this community might have been a result from the influent feeding strategy in which, besides ammonium, nitrite was provided over most of the experiment to prevent limitation in NOB growth in case ammonia

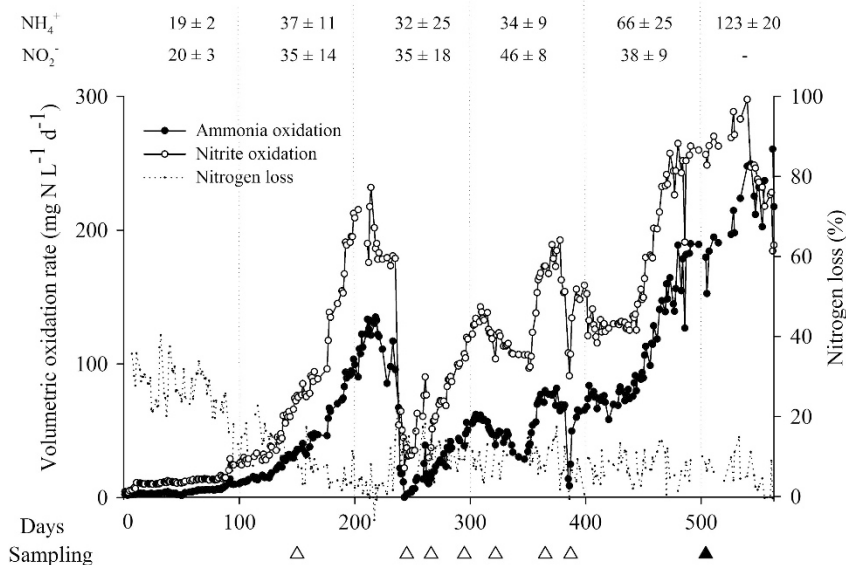


**Figure 1** Nitrification performance ( $\text{mg N L}^{-1} \text{d}^{-1}$ ) and nitrogen loss (%), that is, the amount of removed  $\text{NH}_4^+\text{-N}$  not recovered as  $\text{NO}_2^-\text{-N}$  or  $\text{NO}_3^-\text{-N}$ , in the thermophilic bioreactor (50 °C) inoculated with thermophilic nitrifying batch enrichments from compost samples. Average influent  $\text{NH}_4^+\text{-N}$  and  $\text{NO}_2^-\text{-N}$  concentrations ( $\text{mg N L}^{-1}$ ,  $n = \pm 70$ , over  $\sim 100$  days) are presented on top of the figure. The white and black triangles indicate the sampling for high-throughput DNA sequencing and transmission electron microscopy, respectively.

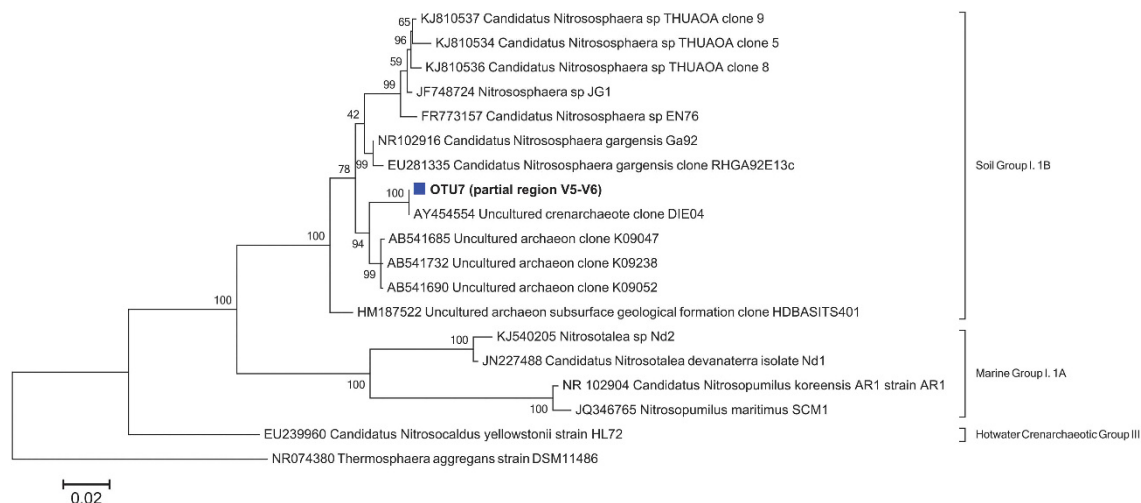


**Figure 2** Phylogenetic relationships between the archaeal 16S rRNA gene sequence (OTU7) of the thermophilic nitrifying reactor biomass and all described AOA cultures or isolates, as well as relevant environmental clone sequences. OTU7 belongs to the group 1.1b of Thaumarchaeota (formerly Crenarchaeota). The short (V5–V6) sequence was added after construction of the full-length sequence tree.

oxidation would decrease (Figure 1). Beside the core nitrifiers (OTU1 and OTU7), the most abundant OTUs (>1%) at the end of the experiment appeared to be, among others, OTU2 and OTU3 (*Meiothermus*), OTU4 (*Thermomonas*), OTU5 and OTU8 (*Armatimonadetes*), OTU9 (*Ignavibacterium*) and OTU11 (*Proteobacterium*) (Supplementary Figure S4).

The presence of the described nitrifiers in the biofilm of the thermophilic reactor was confirmed through transmission electron microscopy (Supplementary Table S4). Cells with morphologies identical to *Nitrospira* spp. and ‘*Candidatus Nitrososphaera gargensis*’ were identified. Cells of *Nitrospira* spp. were characterized by a spiral-shaped morphology with a pleomorphic cell appearance, a

wide periplasmic space and a granular cell interior (Ehrich *et al.*, 1995) (Supplementary Table S4). Small, very electron-dense, spherical cells with thick cell wall with visible fimbriae and pili were observed, similar to the ‘*Candidatus Nitrososphaera gargensis*’ AOA characterized by Hatzenpichler *et al.* (2008) (Supplementary Table S4). As the putative AOA cells were observed closely to the *Nitrospira* cells, this suggests the role of the former cells as ammonia oxidizers.

#### Carbon incorporation

The autotrophic nature of the AOA and NOBs during nitrification was investigated by

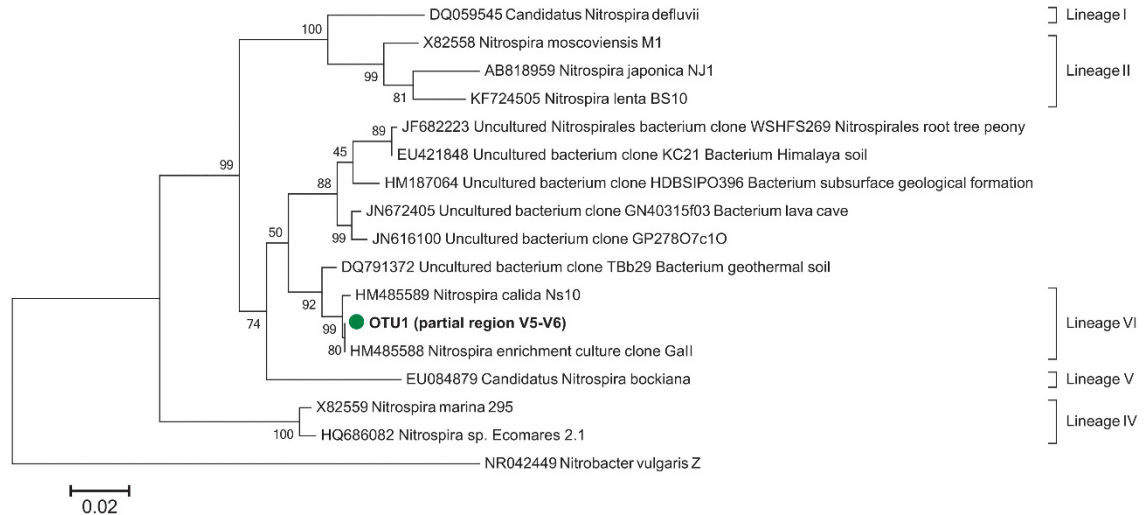


**Figure 3** Phylogenetic relationships between the most dominant *Nitrospira* 16S rRNA gene sequences of the thermophilic nitrifying reactor biomass (OTU1) and all described *Nitrospira* cultures or isolates, as well as relevant environmental clone sequences. The short (V5–V6) sequence was added after construction of the full-length sequence tree.

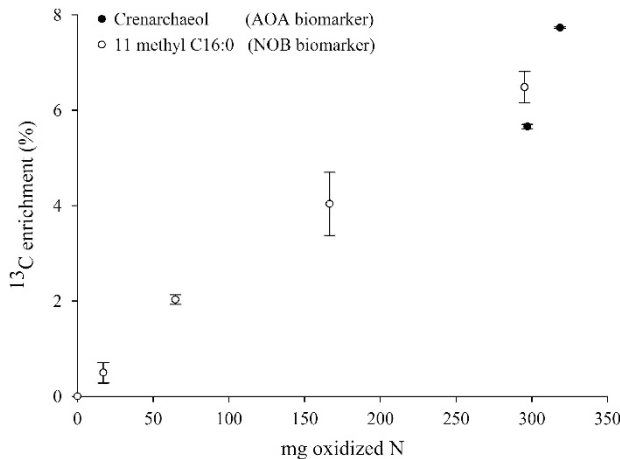


**Figure 4** Relationship between the absolute amount of nitrogen oxidized and the  $^{13}\text{C}$  incorporation in characteristic biomarkers: the biphytane moieties of the GDGTs, more specifically crenarchaeol, as a biomarker for ‘*Candidatus Nitrososphaera gargensis*’ and the 11 methyl C16:0 as a specific phospholipid fatty acid biomarker of *Nitrospira* spp. Data points represent the average replicate extractions ( $n=3$ ), and error bars represent the s.e.

incorporation of  $^{13}\text{C}$ -derived bicarbonate into the characteristic membrane lipids during two sets of incubations, one with  $\text{NH}_4^+$  and another with  $\text{NO}_2^-$ . Isotopic analysis of the biphytane moieties of the characteristic archaeal membrane lipids, GDGTs (glycerol dibiphytanyl glycerol tetraether lipids), was performed for AOAs. The GDGTs were dominated by crenarchaeol, in agreement with culture studies of ‘*Candidatus Nitrososphaera gargensis*’ (Pitcher *et al.*, 2010). The two biphytanes released showed considerable enrichment in  $^{13}\text{C}$  compared with the start of the incubation, pointing at AOA autotrophy (Figure 4). The activity of NOBs was determined by assessing the incorporation of  $^{13}\text{C}$ -labeled bicarbonate into 11-methyl C16:0, a specific

biomarker for moderately thermophilic *Nitrospira* (Lipski *et al.*, 2001; Spieck and Lipski, 2011). The isotopic label was incorporated in the 11-methyl C16:0 phospholipid fatty acid biomarker after a lag time of 3 days at the rate of 0.3% per day during the 21 days of incubation. Interestingly, both for AOAs and NOBs, the  $^{13}\text{C}$  enrichment (%) appeared to be linear with the total amount of nitrogen oxidized (Figure 4), demonstrating that the autotrophic carbon assimilation by AOA and NOB occurred concurrently with the  $\text{NH}_3$  and  $\text{NO}_2^-$  oxidation. Furthermore, the partnership between ‘*Candidatus Nitrososphaera gargensis*’ and *N. calida* was confirmed, as a 26%  $^{13}\text{C}$  enrichment was measured for the *Nitrospira* biomarker at the end of the incubation fed with  $\text{NH}_4^+$ .

#### Physiological characterization

The thermophilic biomass showed specific nitrifying rates up to  $198 \pm 10$  and  $894 \pm 81 \text{ mg N g}^{-1} \text{ VSS per day}$  for  $\text{NH}_3$  and  $\text{NO}_2^-$  oxidation, respectively. Taking into account an average relative abundance of 10% AOAs and 25% NOBs and the simplified assumption that total protein was equally distributed among all organisms in the culture, these rates result in a specific AOA and NOB rate of  $18 \pm 1$  and  $33 \pm 3 \text{ } \mu\text{g N mg}^{-1} \text{ protein h}^{-1}$ , respectively. With respect to the development of biotechnological applications and effective process control strategies, it is important to distinguish the inhibitory effects of  $\text{NH}_4^+$  from those of FA and  $\text{NO}_2^-$  from those of FNA. The thermophilic  $\text{NH}_3$  and  $\text{NO}_2^-$  oxidizers were both sensitive to FA, whereas they were insusceptible to  $\text{NH}_4^+$ . Ammonia oxidation was not inhibited up to  $300 \text{ mg NH}_4^+\text{-N l}^{-1}$  for the batch activity series with low FA, whereas it was inhibited for the series tested at a higher FA, resulting in half-maximal inhibitory concentration ( $\text{IC}_{50}$ ) of  $7.5 \text{ mg NH}_3\text{-N l}^{-1}$  (Figure 5a).

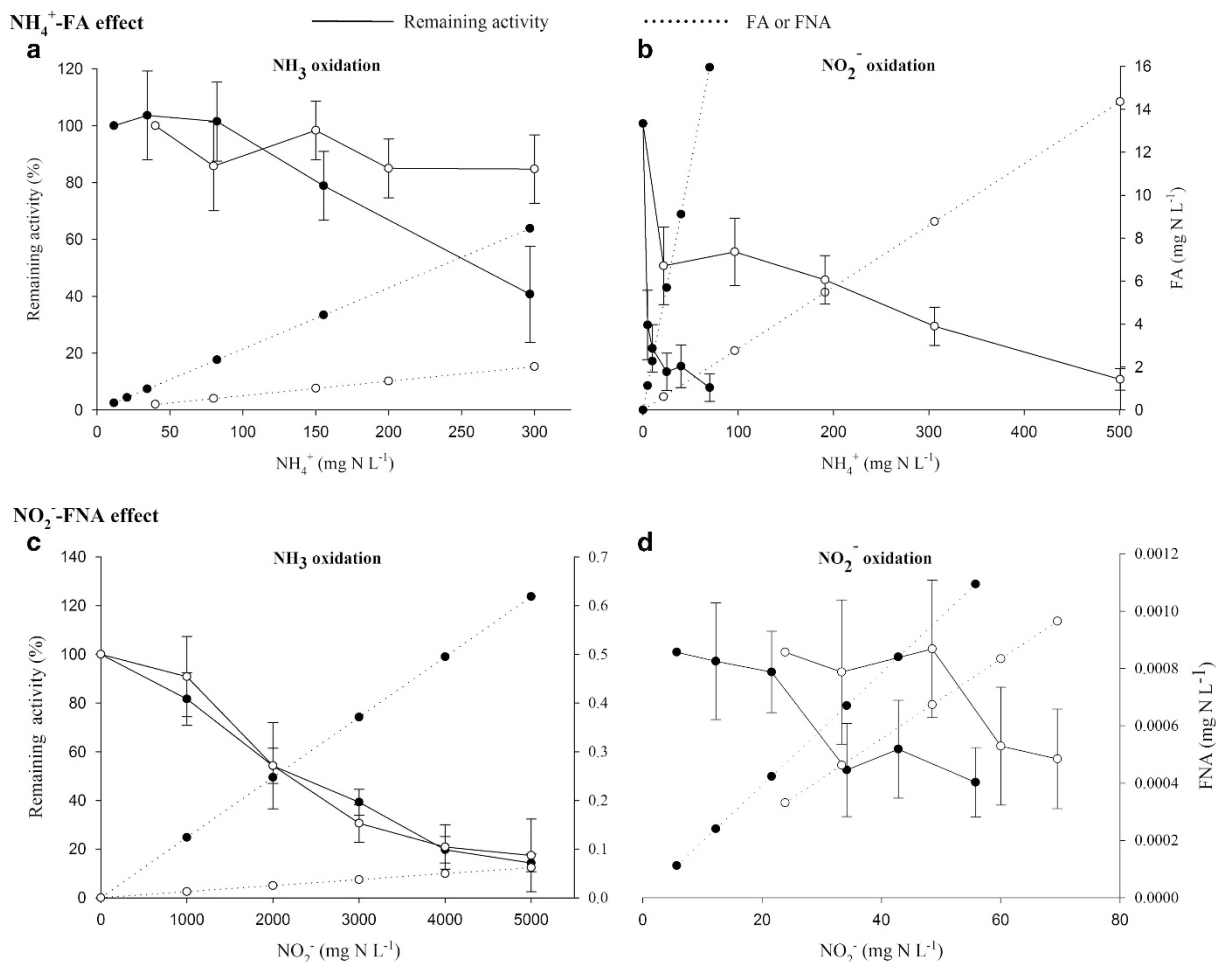


**Figure 5** Effect of ammonium/FA and nitrite/FNA levels on thermophilic ammonia (a, c) and nitrite (b, d) oxidation. Each panel represents two complementary batch activity experiments (filled and empty circles) with full lines depicting the remaining activity, whereas the dotted lines display the corresponding FA/FNA levels per test. Data points represent the average replicate tests ( $n=6$ ), and error bars represent the s.e.

Interestingly, no complete inhibition of ammonia oxidation was observed at up to 80 mg  $\text{NH}_3\text{-N l}^{-1}$  (Supplementary Figure S5). A stable FA ammonia inhibition of  $64 \pm 5\%$  was measured from 8.5 mg  $\text{NH}_3\text{-N l}^{-1}$  onwards (Supplementary Figure S5). Nitrite oxidation was slightly more sensitive for FA with an  $\text{IC}_{50}$  of 5.0 mg  $\text{NH}_3\text{-N l}^{-1}$  (Figure 5b). Regarding  $\text{NO}_2^-/\text{FNA}$  inhibition, ammonia oxidizers were clearly inhibited by  $\text{NO}_2^-$  and not by FNA. Both the series with high and low FNA gave the same inhibition response with increasing  $\text{NO}_2^-$  concentrations (Figure 5c). Sensitivity was, however, very low, characterized with an  $\text{IC}_{50}$  of 2117 mg  $\text{NO}_2^- \text{N l}^{-1}$ . In contrast, the NOBs were extremely sensitive to FNA and not to  $\text{NO}_2^-$  with an  $\text{IC}_{50}$  of 0.0010 mg  $\text{HNO}_2\text{-N l}^{-1}$  (Figure 5d). Lowering FNA while applying the same  $\text{NO}_2^-$  concentrations eliminated the inhibitory effect. Nitrate inhibition of nitrite oxidation was also observed ( $\text{IC}_{50}$  360 mg  $\text{NO}_3^- \text{N l}^{-1}$ ) (Supplementary Figure S6).

Thermophilic  $\text{NH}_3$  oxidation showed a pH optimum at pH 7, maintaining  $>70\%$  of its activity within the tested pH range (pH 6–8) (Figure 6).

Although the bioreactor was controlled between pH 6.8 and 7.2, it showed increasing  $\text{NO}_2^-$  oxidation at lower pH, given low FNA concentrations (Figure 6). Ammonia oxidation showed a broad temperature optimum (45–55 °C), whereas nitrite oxidation showed a clear optimal activity at the reactor temperature (50 °C). Thermophilic  $\text{NH}_3$  oxidation could be inhibited by the conventional nitrification inhibitor allylthiourea with an  $\text{IC}_{50/100}$  of 3.5/8.8 mM and the AOA-specific inhibitor carboxy-PTIO (2-(4-Carboxyphenyl)-4,4,5,5-tetramethylimidazole-1-oxyl-3-oxide) with an  $\text{IC}_{50/100}$  of 63/117  $\mu\text{M}$  (Supplementary Figure S7).

## Discussion

In this study, the enrichment of coupled autotrophic thermophilic ammonia and nitrite oxidizers from compost was achieved followed by the successful operation of a thermophilic nitrifying bioreactor, opening up opportunities for nitrogen removal in warm wastewater.

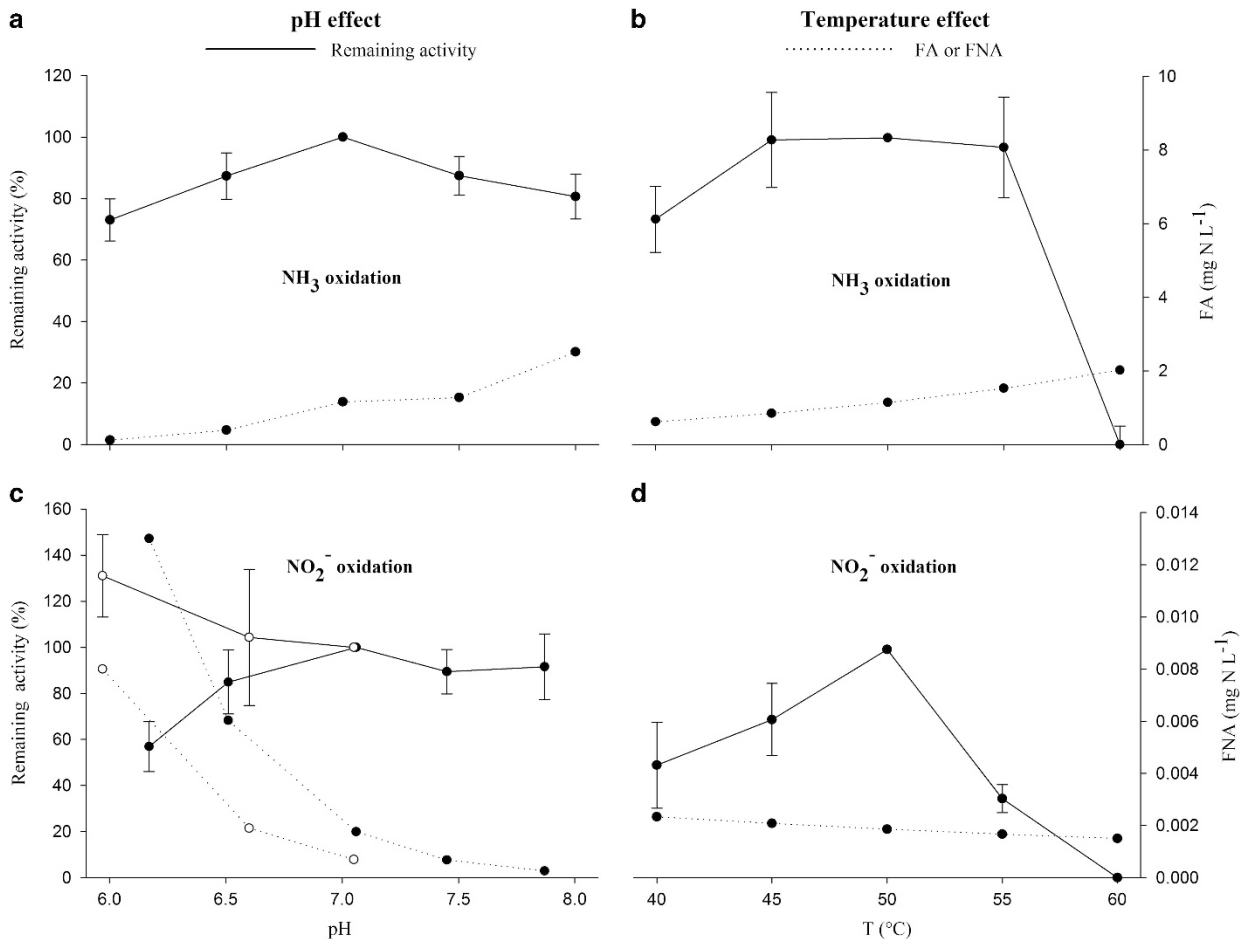


**Figure 6** Effect of pH and temperature on thermophilic ammonia (a, b) and nitrite (c, d) oxidation. Data points represent the average replicate tests ( $n=6$ ), and error bars represent the s.e.

The thermophilic nitrifying community in the bioreactor consisted of an AOA and NOB closely related to ‘*Candidatus Nitrososphaera gargensis*’ and *N. calida*. Interestingly, the same coexistence was found in nature as both were originally isolated from the Garga hot spring (Russia) (Hatzenpichler *et al.*, 2008; Lebedeva *et al.*, 2011). In contrast to the oligotrophic nature of these geothermal springs, this study enriched nitrifiers from aerobic compost, a nutrient-rich high-temperature anthropogenic environment. Although many archaeal *amoA* genes (Maeda *et al.*, 2011; Zeng *et al.*, 2011) and even ‘*Candidatus Nitrososphaera gargensis*’-like sequences (Yamamoto *et al.*, 2011; Oishi *et al.*, 2012) were detected during composting processes, so far no autotrophic thermophilic nitrifiers were enriched from compost. Only a heterotrophic AOB growing at 50 °C related to *Bacillus halodurans* was isolated previously from animal waste composting (Shimaya and Hashimoto, 2011). As the two compost piles that originally contained appreciable nitrate levels developed thermophilic ammonia oxidation, whereas all compost yielded nitrite oxidation, the

presence of nitrate can lead to a smart selection of compost type for further studies focusing on thermophilic AOAs. The presence of the described core nitrifiers in the bioreactor was, furthermore, linked with their activity and functionality. Incorporation of <sup>13</sup>C-labeled bicarbonate was observed into crenarchaeol and 11-methyl C16:0, characteristic membrane lipids for ‘*Candidatus Nitrososphaera gargensis*’ (Pitcher *et al.*, 2010) and *Nitrospira* (Lipski *et al.*, 2001), respectively. Although the carbon assimilation confirmed the autotrophic activity of the studied nitrifiers, it does not exclude the presence of other, unknown autotrophic or heterotrophic nitrifiers. An abundant cell type, embedded in a dense biofilm structure, could not be identified. Together with the observed delay/heterogeneity of the AOAs presence over time (Supplementary Figure S3), this could suggest that an uncharacterized ammonia-oxidizing organism was also present, as was recently observed in reactors with low dissolved oxygen concentrations (Fitzgerald *et al.*, 2015). The linearity of the nitrogen oxidation and the <sup>13</sup>C enrichment in the stable isotope experiment (Figure 4), however,

suggest that '*Candidatus Nitrososphaera gargensis*' and *N. calida* were important thermophilic nitrifiers in the biomass community.

The physiological characterization revealed that the specific oxidation rates of both AOA ( $18 \pm 1 \mu\text{g N mg}^{-1} \text{protein h}^{-1}$ ) and NOBs ( $33 \pm 3 \mu\text{g N mg}^{-1} \text{protein h}^{-1}$ ) were in the same order of magnitude as related nitrifiers. In particular, the specific rates for AOA range from 11 to  $24 \mu\text{g N mg}^{-1} \text{protein h}^{-1}$  (Kim *et al.*, 2012), whereas reported rates for *Nitrospira* spp. range between 16 and  $42 \mu\text{g N mg}^{-1} \text{protein h}^{-1}$  (Nowka *et al.*, 2015). Interesting differences in substrate/product tolerances were observed. Until now, data concerning  $\text{NH}_4^+/\text{NH}_3$  inhibition on (thermophilic) AOA has been limited attributing the inhibitory effect to  $\text{NH}_4^+$  without excluding FA inhibition. However, with respect to biotechnological applications and the development of effective process control strategies, this distinction can be of great importance and was determined in this study. The '*Candidatus Nitrososphaera gargensis*'-like AOA in the thermophilic nitrifying bioreactor appeared to be insensitive to  $\text{NH}_4^+$ , and could maximally be inhibited by  $63 \pm 5\%$  from  $8.5 \text{ mg NH}_3\text{-N l}^{-1}$  (Figure 5 and Supplementary Figure S5). At a neutral pH and a temperature of 50 °C, this inhibition corresponds to a  $\text{NH}_4^+$  concentration of  $300 \text{ mg NH}_4^+\text{-N l}^{-1}$ . This concentration is 7 times higher than the inhibitory  $\text{NH}_4^+$  concentration reported for '*Candidatus Nitrososphaera gargensis*' (Hatzenpichler *et al.*, 2008). The higher FA tolerance could be attributed to the fact that the AOA in this study originated from nutrient-rich compost in contrast with oligotrophic geothermal springs. Indeed, the AOA detected in cattle manure compost by Oishi *et al.* (2012) also showed a higher tolerance toward media with a higher  $\text{NH}_4^+$  concentration. The thermophilic NOBs in the bioreactor of our study were also sensitive to FA and insensitive to  $\text{NH}_4^+$ , but the higher sensitivity ( $\text{IC}_{50}$  of  $5.0 \text{ mg NH}_3\text{-N l}^{-1}$ ) could allow a selective NOB inhibition based on FA. Furthermore, the AOA were insensitive to FNA, whereas the NOBs were extremely sensitive to FNA ( $\text{IC}_{50}$  of  $0.0010 \text{ mg HNO}_2\text{-N l}^{-1}$ ). Both the insensitivity of AOA for FNA and the high sensitivity of NOB for FA and FNA suggest that a selective NOB inhibition could be easily established in the described thermophilic nitrifying community, enabling the development of more cost-effective nitrogen removal processes, such as nitrification/denitrification or deammonification.

Until now, the main thermophilic nitrogen removal mechanism was assumed to be ammonia stripping and nitrogen assimilation into biomass (Abeynayaka and Visvanathan, 2011a). Development of thermophilic biotechnology for nitrogen removal is necessary, as ammonia stripping transfers the problem to the gas phase, and no sufficient nitrogen removal can be reached based on assimilation. Besides eliminating cooling requirements, thermophilic nitrogen removal also lowers sludge

production and confers better settling properties (Suvilampi and Rintala, 2003). These advantages apply not only to warm wastewaters but also to wastewaters on sites with excess heat available. A few lab-scale studies have explored the potential of thermophilic nitrification for wastewater treatment, but achieved no more than 40–42.5 °C (Shore *et al.*, 2012; Courtens *et al.*, 2014a). Thus far, this is the first study describing a thermophilic nitrifying bioreactor at 50 °C. Although challenges such as the effect of carbon on the autotrophic/heterotrophic competition and the coupling of nitrification with a reductive nitrogen removal process (denitrification, anammox) have to be addressed to enable implementation, this study paves the way for thermophilic nitrogen removal.

## Conflict of Interest

The authors declare no conflict of interest.

## Acknowledgements

ENPC and SEV were supported as doctoral candidate (Aspirant) and postdoctoral fellow, respectively, by the Research Foundation Flanders (FWO-Vlaanderen). RV-V was supported as a postdoctoral fellow from the Belgian Science Policy Office (BELSPO). ES was funded by the DFG (SP 667/7-2). The reactor equipment used for this study was provided through Global Water Engineering NV and the King Baudouin Foundation. We thank Stefanie Delbeke, Luc De Clercq, Fabian De Wilde (OWS NV) and Marc Verhofstede (Humus Sprl.) for providing the compost samples. We also thank Elke Woelken for assistance with transmission electron microscopy, Marianne Baas and Monique Verweij for lipid isotope analysis and José M Carvajal-Arroyo and Tom Vandekerckhove for assistance with the reactor experiment.

## References

- Abeynayaka A, Visvanathan C. (2011a). Performance comparison of mesophilic and thermophilic aerobic sidestream membrane bioreactors treating high strength wastewater. *Bioresour Technol* **102**: 5345–5352.
- Abeynayaka A, Visvanathan C. (2011b). Mesophilic and thermophilic aerobic batch biodegradation, utilization of carbon and nitrogen sources in high-strength wastewater. *Bioresour Technol* **102**: 2358–2366.
- Anthonisen AC, Loehr RC, Prakasam TBS, Srinath EG. (1976). Inhibition of nitrification by ammonia and nitrous-acid. *J Water Pollut Control Fed* **48**: 835–852.
- Baker BJ, Lesniewski RA, Dick GJ. (2012). Genome-enabled transcriptomics reveals archaeal populations that drive nitrification in a deep-sea hydrothermal plume. *ISME J* **6**: 2269–2279.
- Bohorquez LC, Delgado-Serrano L, Lopez G, Osorio-Forero C, Klepac-Ceraj V, Kolter R *et al.* (2012). In-depth characterization via complementing culture-independent approaches of the microbial community

- in an acidic hot spring of the Colombian Andes. *Microb Ecol* **63**: 103–115.
- Camarinha-Silva A, Jáuregui R, Chaves-Moreno D, Oxley APA, Schaumburg F, Becker K *et al.* (2014). Comparing the anterior nare bacterial community of two discrete human populations using Illumina amplicon sequencing. *Environ Microbiol* **16**: 2939–2952.
- Courtens ENP, Boon N, De Schryver P, Vlaeminck SE. (2014a). Increased salinity improves the thermotolerance of mesophilic nitrification. *Appl Microbiol Biotechnol* **98**: 4691–4699.
- Courtens ENP, Vlaeminck SE, Vilchez-Vargas R, Verliefe A, Jauregui R, Pieper DH *et al.* (2014b). Trade-off between mesophilic and thermophilic denitrification: rates vs. sludge production, settleability and stability. *Water Res* **63**: 234–244.
- de la Torre JR, Walker CB, Ingalls AE, Konneke M, Stahl DA. (2008). Cultivation of a thermophilic ammonia oxidizing archaeon synthesizing crenarchaeol. *Environ Microbiol* **10**: 810–818.
- Dionisi HM, Layton AC, Harms G, Gregory IR, Robinson KG, Sayler GS. (2002). Quantification of nitrosomonas oligotropha-like ammonia-oxidizing bacteria and Nitrospira spp. from full-scale wastewater treatment plants by competitive PCR. *Appl Environ Microbiol* **68**: 245–253.
- Dodsworth JA, Hungate BA, Hedlund BP. (2011). Ammonia oxidation, denitrification and dissimilatory nitrate reduction to ammonium in two US Great Basin hot springs with abundant ammonia-oxidizing archaea. *Environ Microbiol* **13**: 2371–2386.
- Edwards TA, Calica NA, Huang DA, Manoharan N, Hou W, Huang L *et al.* (2013). Cultivation and characterization of thermophilic Nitrospira species from geothermal springs in the US Great Basin, China, and Armenia. *FEMS Microbiol Ecol* **85**: 283–292.
- Ehrich S, Behrens D, Lebedeva E, Ludwig W, Bock E. (1995). A new obligately chemolithoautotrophic, nitrite-oxidizing bacterium, Nitrospira moscoviensis sp. nov. and its phylogenetic relationship. *Arch Microbiol* **164**: 16–23.
- Fitzgerald CM, Camejo P, Oshlag JZ, Noguera DR. (2015). Ammonia-oxidizing microbial communities in reactors with efficient nitrification at low-dissolved oxygen. *Water Res* **70**: 38–51.
- Galloway JN, Winiwarter W, Leip A, Leach AM, Bleeker A, Erisman JW. (2014). Nitrogen footprints: past, present and future. *Environ Res Lett* **9**: 1–11.
- Hatzenpichler R, Lebedeva EV, Spieck E, Stoecker K, Richter A, Daims H *et al.* (2008). A moderately thermophilic ammonia-oxidizing crenarchaeote from a hot spring. *Proc Natl Acad Sci USA* **105**: 2134–2139.
- Huygens D, Roobroeck D, Cosyn L, Salazar F, Godoy R, Boeckx P. (2011). Microbial nitrogen dynamics in south central Chilean agricultural and forest ecosystems located on an Andisol. *Nutr Cycl Agroecosyst* **89**: 175–187.
- Jukes TH, Cantor CR. (1969). Evolution of protein molecules. In: Munro HN (ed), *Mammalian Protein Metabolism*. Academic Press: New York, NY, USA, pp 21–132.
- Kim J-G, Jung M-Y, Park S-J, Rijpstra WIC, Damste JSS, Madsen EL *et al.* (2012). Cultivation of a highly enriched ammonia-oxidizing archaeon of thaumarchaeotal group I.1b from an agricultural soil. *Environ Microbiol* **14**: 1528–1543.
- Kuai LP, Verstraete W. (1998). Ammonium removal by the oxygen-limited autotrophic nitrification-denitrification system. *Appl Environ Microbiol* **64**: 4500–4506.
- Kurian R, Acharya C, Nakhla G, Bassi A. (2005). Conventional and thermophilic aerobic treatability of high strength oily pet food wastewater using membrane-coupled bioreactors. *Water Res* **39**: 4299–4308.
- Lebedeva EV, Alawi M, Fiencke C, Namsaraev B, Bock E, Spieck E. (2005). Moderately thermophilic nitrifying bacteria from a hot spring of the Baikal rift zone. *FEMS Microbiol Ecol* **54**: 297–306.
- Lebedeva EV, Off S, Zumbraegel S, Kruse M, Shagzhina A, Luecker S *et al.* (2011). Isolation and characterization of a moderately thermophilic nitrite-oxidizing bacterium from a geothermal spring. *FEMS Microbiol Ecol* **75**: 195–204.
- Lebedeva EV, Hatzenpichler R, Pelletier E, Schuster N, Hauzmayer S, Bulaev A *et al.* (2013). Enrichment and genome sequence of the group I.1a ammonia-oxidizing Archaeon "Ca. Nitrosotenuis uzonensis" representing a clade globally distributed in thermal habitats. *PLoS One* **8**: e80835.
- Lengger SK, Lipsewers YA, de Haas H, Damste JSS, Schouten S. (2014). Lack of C-13-label incorporation suggests low turnover rates of thaumarchaeal intact polar tetraether lipids in sediments from the Iceland shelf. *Biogeosciences* **11**: 201–216.
- Li H, Mu B-Z, Jiang Y, Gu J-D. (2011). Production processes affected prokaryotic amoA gene abundance and distribution in high-temperature petroleum reservoirs. *Geomicrobiol J* **28**: 692–704.
- Lipski A, Spieck E, Makolla A, Altendorf K. (2001). Fatty acid profiles of nitrite-oxidizing bacteria reflect their phylogenetic heterogeneity. *Syst Appl Microbiol* **24**: 377–384.
- Lopez-Vazquez CM, Kubare M, Saroj DP, Chikamba C, Schwarz J, Daims H *et al.* (2014). Thermophilic biological nitrogen removal in industrial wastewater treatment. *Appl Microbiol Biotechnol* **98**: 945–956.
- Maeda K, Hanajima D, Toyoda S, Yoshida N, Morioka R, Osada T. (2011). Microbiology of nitrogen cycle in animal manure compost. *Microb Biotechnol* **4**: 700–709.
- Marks CR, Stevenson BS, Rudd S, Lawson PA. (2012). Nitrospira-dominated biofilm within a thermal artesian spring: a case for nitrification-driven primary production in a geothermal setting. *Geobiology* **10**: 457–466.
- Nisbet EG, Sleep NH. (2001). The habitat and nature of early life. *Nature* **409**: 1083–1091.
- Nowka B, Daims H, Spieck E. (2015). Comparison of oxidation kinetics of nitrite-oxidizing bacteria: nitrite availability as a key factor in niche differentiation. *Appl Environ Microbiol* **81**: 745–753.
- Oishi R, Tada C, Asano R, Yamamoto N, Suyama Y, Nakai Y. (2012). Growth of ammonia-oxidizing archaea and bacteria in cattle manure compost under various temperatures and ammonia concentrations. *Microb Ecol* **63**: 787–793.
- Pitcher A, Rychlik N, Hopmans EC, Spieck E, Rijpstra WIC, Ossebaar J *et al.* (2010). Crenarchaeol dominates the membrane lipids of Candidatus Nitrososphaera gargensis, a thermophilic Group I. 1b Archaeon. *ISME J* **4**: 542–552.
- Reigstad LJ, Richter A, Daims H, Urich T, Schwark L, Schleper C. (2008). Nitrification in terrestrial hot

- springs of Iceland and Kamchatka. *FEMS Microbiol Ecol* **64**: 167–174.
- Schouten S, Hugué C, Hopmans EC, Kienhuis MVM, Damste JSS. (2007). Analytical methodology for TEX86 paleothermometry by high-performance liquid chromatography/atmospheric pressure chemical ionization-mass spectrometry. *Anal Chem* **79**: 2940–2944.
- Shimaya C, Hashimoto T. (2011). Isolation and characterization of novel thermophilic nitrifying *Bacillus* sp. from compost. *Soil Sci Plant Nutr* **57**: 150–156.
- Shore JL, M'Coy WS, Gunsch CK, Deshusses MA. (2012). Application of a moving bed biofilm reactor for tertiary ammonia treatment in high temperature industrial wastewater. *Bioresour Technol* **112**: 51–60.
- Sorokin DY, Vejmelkova D, Lucker S, Streshinskaya GM, Rijpstra WI, Sinninghe Damste JS et al. (2014). Nitrolancea hollandica gen. nov., sp. nov., a chemolithoautotrophic nitrite-oxidizing bacterium isolated from a bioreactor belonging to the phylum Chloroflexi. *Int J Syst Evol Microbiol* **64**: 1859–1865.
- Spear JR, Barton HA, Robertson CE, Francis CA, Pace NR. (2007). Microbial community biofabrics in a geothermal mine adit. *Appl Environ Microbiol* **73**: 6172–6180.
- Spieck E, Lipski A. (2011). Cultivation, growth physiology, and chemotaxonomy of nitrite-oxidizing bacteria. *Methods Enzymol* **486**: 109–130.
- Steffen W, Richardson K, Rockström J, Cornell SE, Fetzer I, Bennett EM et al. (2015). Planetary boundaries: guiding human development on a changing planet. *Science* **347**: 1259855.
- Suvilampi J, Rintala J. (2003). Thermophilic aerobic wastewater treatment, process performance, biomass characteristics, and effluent quality. *Rev Environ Sci Biotechnol* **2**: 35–51.
- Tamura K, Peterson D, Peterson N, Stecher G, Nei M, Kumar S. (2011). MEGA5: molecular evolutionary genetics analysis using maximum likelihood, evolutionary distance, and maximum parsimony methods. *Mol Biol Evol* **28**: 2731–2739.
- Tourna M, Freitag TE, Nicol GW, Prosser JI. (2008). Growth, activity and temperature responses of ammonia-oxidizing archaea and bacteria in soil microcosms. *Environ Microbiol* **10**: 1357–1364.
- Vlaeminck SE, Hay AG, Maignien L, Verstraete W. (2011). In quest of the nitrogen oxidizing prokaryotes of the early Earth. *Environ Microbiol* **13**: 283–295.
- Wang SF, Xiao X, Jiang LJ, Peng XT, Zhou HY, Meng J et al. (2009). Diversity and abundance of ammonia-oxidizing archaea in hydrothermal vent chimneys of the Juan de Fuca Ridge. *Appl Environ Microbiol* **75**: 4216–4220.
- Ward BB, Arp DJ, Klotz MG. (2011). *Nitrification*. ASM Press: Washington, DC, USA.
- Weidler GW, Gerbl FW, Stan-Lotter H. (2008). Crenarchaeota and their role in the nitrogen cycle in a subsurface radioactive thermal spring in the Austrian central Alps. *Appl Environ Microbiol* **74**: 5934–5942.
- Yamamoto N, Asano R, Yoshii H, Otawa K, Nakai Y. (2011). Archaeal community dynamics and detection of ammonia-oxidizing archaea during composting of cattle manure using culture-independent DNA analysis. *Appl Microbiol Biotechnol* **90**: 1501–1510.
- Yi YS, Kim S, An S, Choi SI, Choi E, Yun Z. (2003). Gas analysis reveals novel aerobic deammonification in thermophilic aerobic digestion. *Water Sci Technol* **47**: 131–138.
- Zeng G, Zhang J, Chen Y, Yu Z, Yu M, Li H et al. (2011). Relative contributions of archaea and bacteria to microbial ammonia oxidation differ under different conditions during agricultural waste composting. *Bioresour Technol* **102**: 9026–9032.

Supplementary Information accompanies this paper on The ISME Journal website (<http://www.nature.com/ismej>)